

Defect Free Nonporous Polyurethane Membrane; Preparation, Characterization and Performance in Gas Separation

Aiza Shoukat^{a,*} Mohamed, E. A. Ali^{b,*} Mohammed Zuber^a

^aChemistry Department. Government Collage University Faisalabad, Pakistan

^bDesalination unit, Hydrochemistry Department., Desert Research Center, Cairo, Egypt

*Department of Chemical engineering. University of Waterloo, Ontario, Canada

Corresponding author, aizachemist@yahoo.com

Department of Applied Chemistry Government Collage University ,Faisalabad

Abstract

This article aims to fabrication of Polycaprolactone based Polyurethane as a gas barrier membranes. To enhance the membrane performance, diisocyanates and chain extender were incorporated into a polyurethane matrix. Different synthesis conditions were investigated and the membrane morphologies were characterized by FTIR, TGA, DSC, and AFM. The Permeation properties of the prepared membranes were studied as a function of processing methodology. The results show that polymers with high molecular weight and sonication instead of electrical stirring gave significantly better barrier properties. The permeance of gases increase with increase of temperature resulting in the reduction of CO₂/CH₄ selectivity in 1,6-Hexamethylene diisocyanate (HDI) based Polyurethane membranes. But, the CO₂/N₂ selectivity in 4,4'-methylene dicyclohexyl diisocyanate (H₁₂MDI) PUs is little bit higher. Because the permeation of more condensable CO₂ gas in comparison to nonpermeable nitrogen increase in more phase separated structures, therefore effect of the solution selectivity in the separation of condensable and non-condensable gases increase and this membrane show the higher CO₂/N₂ selectivity in comparison to the HDI system.

Keywords, polyurethane, Gas separation, Polyol, membrane selectivity.

Highlights

The polyurethane membranes are ecofriendly and can easily be degraded

Gas separation with temperature and pressure differences across the membrane.

Molecular exchange flow by the thermal transpiration in the non-porous membrane.

Low cost membrane is available for gas separation.

1. Introduction

The removal of undesirable species from certain gas streams by the use of gas absorption is of major industrial and environmental importance. Membrane technologies play a significant role in meeting these needs. Typically, one expects membranes to transmit small molecules more rapidly than larger ones; however, there are numerous applications where it would be advantageous to have membranes that preferentially transmit certain larger molecules faster than smaller ones, i.e., the reverse of the expected size selectivity. Barrer¹ and van Amerongen² contributed to the foundations for modern day gas permeation and separation theories. Baker et al. designed organic vapor separation membranes using various silicon based rubbery materials³. Depending on the application requirements, dense polymeric membranes can be fabricated using glassy or rubbery materials via material design and hybridization. Over the past 20 years, membrane materials have evolved from simple polymers, like cellulose acetate⁴, polysulfones⁵, etc., to well-designed polymers like thermally rearranged polymers, polymers with intrinsic microporosity, fully amorphous polyether rubbers, etc. Park et al. discovered a class of polybenzoxadole that could be thermally rearranged to form materials that facilitate the diffusion of smaller gas penetrants⁶.

The solution-diffusion theory proposed by Thomas Graham is widely used to explain gas transport in non-porous, dense polymeric membranes. According to their theories, gas permeation occurs by sorption of a gas into the upstream surface of the membrane material, then molecular diffusion through the polymer matrix, and subsequent “evaporation” of the gas from the downstream surface of the membrane. Consequently, gas permeation reflects a combination of thermodynamic factors like condensability of the gas and its interaction with the polymer segments plus kinetic factors that are largely governed by the size of the penetrant, polymer segmental mobility and packing, or free volume. Dissolved penetrant molecules execute diffusional “jumps” from one free volume element, i.e., the space between polymer chains, to another. However, the permeation process involves the sorption step as well as diffusion, and the extent of sorption of a gas typically depends on the interaction of the penetrant and the polymer. An effective approach to fabricate CO₂-selective polymeric membranes is to incorporate high CO₂ affinity moieties like ether oxygen⁷ moieties into a polymeric host. Molecules like CO₂ are

acidic in nature and can interact with polar ether oxygen via dipole interactions. As a result, more CO₂ molecules permeate across the material when compared to other gas molecules like hydrogen (H₂), nitrogen (N₂) and methane (CH₄).

Polyurethane systems have also attracted attention for their barrier-like properties. Polyurethanes are inherently versatile and can be processed into a wide variety of products such as fibers, foams, adhesives and coatings⁸. The nature of a micro-phase separation, which is due to a difference in polarity and the thermodynamic incompatibility of the two phases, allows these polymers to be subdivided into a soft and hard phase⁹. The soft segment is generally composed of long flexible polyester or polyether units and provides the elastomeric properties of the polymer¹⁰. The hard phase or second block of the co-polymer is based on isocyanate and triol or diol chain extenders. The hard phase is in an amorphous glassy state or in a crystalline state with hydrogen bonding within the hard segments, and will act as a physical crosslink¹¹. The alternating blocks and the variety of monomers used to synthesize the co-polymer structure permits tailoring the properties of these thermoplastic polyurethanes^{12,13}. The addition of PCL (polyol) into these systems allows for enhanced control of their physical properties. PUs are usually composed of a polyether or polyester soft segment and a hard segment. They usually have a micro-phase separated structure due to the incompatibility between the soft and hard segments.

The effect of diisocyanate on the gas permeation properties of PU based membranes was studied by using two types of aliphatic diisocyanate: 4, 4'-methylene dicyclohexyl diisocyanate (H₁₂MDI) and hexamethylene diisocyanate (HDI). The effect of polyol on gas permeation properties of PU membranes was also tested by means of Polycaprolactone (PCL). All polyols had the same molecular weight of 2000 g/mol. In this study we investigate the effect of processing on the gas barrier properties of polyurethane membranes. In particular we compare the effects of hard segment on the permeability and selectivity of different gases.

2. Experimental

2.1. Materials

The chemicals used in this study are of analytical grade like 4,4'-methylene dicyclohexyl diisocyanate (H₁₂MDI), 1,6-Hexamethylene diisocyanate (HDI), 1,4-butane diol (1,4-BD) as

chain extender, dibutyltin dilaurate (DBTDL) as catalyst and tetrahydrofuran (THF) dimethyl formamide (DMF) as solvents were purchased from Sigma Chemical Co. (Saint. Louis, MO, USA). Poly (caprolactone) diol CAPA 2200A (M.w 2000) was kindly gifted by Perstorp polyols (Solvay chemicals),Inc. Toledo, Ohio.

2.2.Synthesis of Polyurethane membranes:

The air bubbles and water vapors were removed from polyol by drying at 80°C in vacuum for 24 h before use that may otherwise interfere with the isocyanate reactions. Firstly; the PU prepolymer was synthesized by reaction of 4, 4'-methylene dicyclohexyl diisocyanate (H₁₂MDI) with Poly (caprolactone) diol to obtain isocyanate (NCO) terminated polyurethane prepolymer. As follow, into a four-necked round bottom flask equipped with mechanical stirrer, heating oil bath, reflux condenser, dropping funnel and argon inlet and outlet, Poly (caprolactone) was placed. The temperature of the oil bath was increased to 60°C. Then (H₁₂MDI) was added and the temperature was then increased to 100°C and continued stirring. In the second step the conversion of the PU prepolymer into the final PU was carried out by adding 1, 4-butane diol (1mole) with continuous stirring for 20 min at 100°C. This entire reaction was carried out under argon atmosphere. The samples were degassed to remove the entrapped air bubbles for further analysis. The bubble free polymer solution was cast on clean glass plates and incubated at 90 °C for 24 h to allow the evaporation of the solvent. The scheme is shown in figure1.

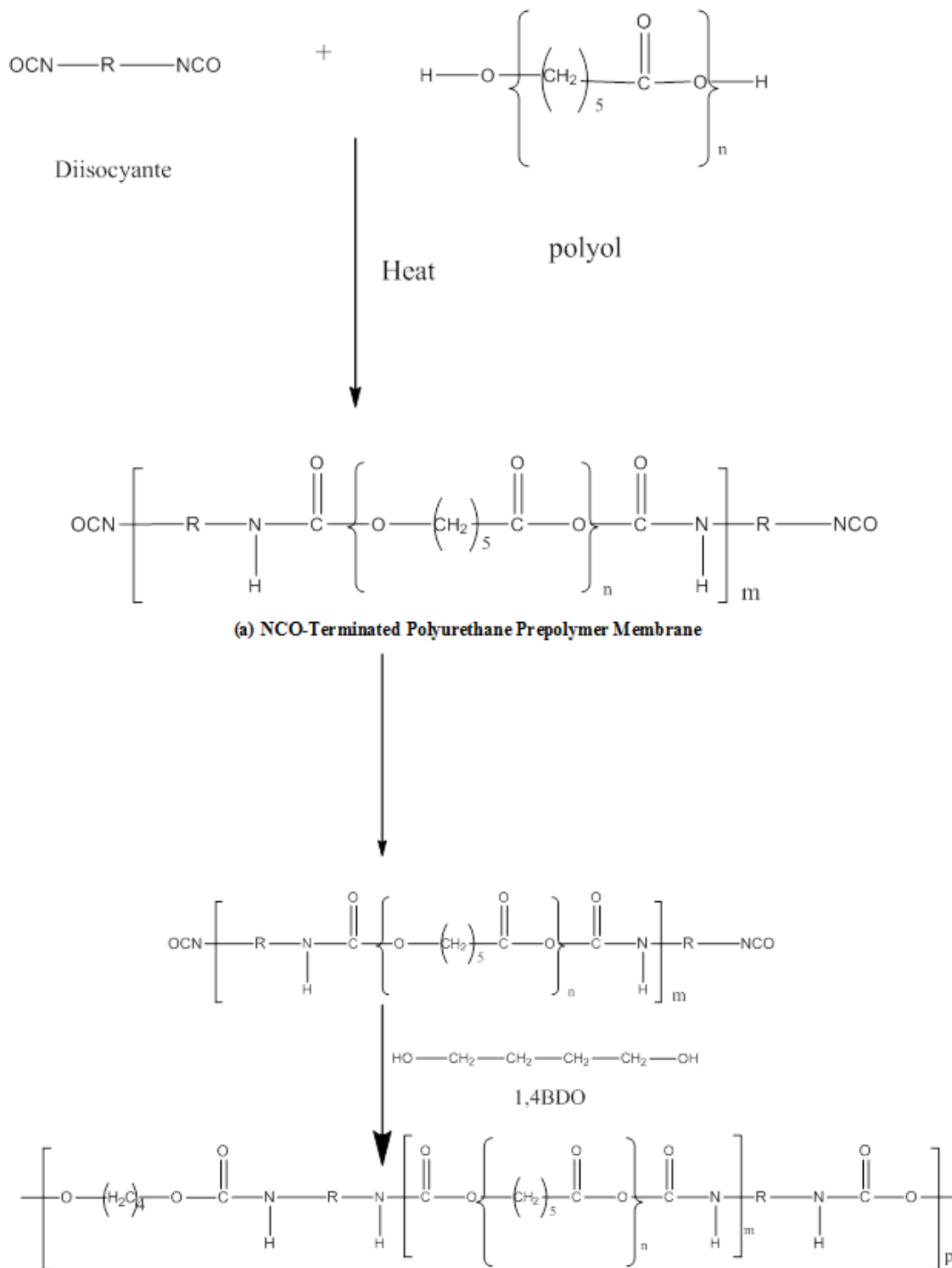


Fig1 schematic scheme of polyurethane membrane

2.3. Characterization

2.3.1. Molecular characterization:

Molecular structure of the synthesized PU membrane using PCL was confirmed using Fourier Transform Infrared (FT-IR) spectroscopy in the range of 500–4000 cm^{-1} . FT-IR scans of the prepared copolymer samples were obtained in the transmission mode using a Shimadzu 80900 Fourier Transform Infra-red (FT-IR) spectrometer. A Fourier transform infrared (FTIR) spectrum of the PU prepolymer was obtained to confirm the progress of reaction (Fig1). The reaction was monitored by Fourier transform infrared (FTIR) spectroscopy technique.

2.3.2. Membrane swelling property:

Small pieces of weighed PU membranes were kept immersed in pure water, Since the membranes were found to achieve equilibrium swelling within 24 h, then the membranes were taken out and their weights were measured immediately after wiping out the surface liquid by soft tissue paper. The following mathematical equation was used to calculate the quantity of water absorbed.

$$\text{Water absorbance (\%)} = \frac{W_w - W_d}{W_d} \times 100$$

W_w and W_d are the weight of wet and dry membranes, respectively.

2.3.3. Thermal analysis:

. In this study, differential scanning calorimeter (DSC 2920) was employed to measure the thermal properties. Each sample (5–10 mg) was scanned from 60 to 250 °C at a scanning rate of 10°C/min under a dry nitrogen purge. The thermal stability analyses were done on a thermo gravimetric analyzer (TGA 2040), where thermograms were recorded from room temperature to 550 °C at a heating rate of 10 °C/min under N_2 purge with a flow rate of 50 mL/min.

2.3.4 Tensile strength testing:

The polymer specimens were injection-molded into dog-bone shapes. Their dimensions were determined according to the ASTM D 638 standard method. The length between bench markers (the two marks placed on the specimen and used to measure elongation or strain) was

approximately 5 cm. The exact dimensions of the specimen (width, length and thickness) were measured again before carrying out the testing. The specimen was placed in an Instron model 4301 Universal Testing scheme, using a stretching rate of 5kN until the specimen ruptured. The tensile strength and percent elongation at break was measured.

2.3.5 AFM analysis:

Atomic force microscopy (AFM) analysis was carried out at room temperature with a Nano Wizard AFM (JPK) in contact mode. During the analysis, the topographic and lateral force images were recorded simultaneously

2.4. Membrane performance in gas permeability

The permeability of oxygen, nitrogen, methane and carbon dioxide were determined using a constant pressure/variable volume method at different pressure and temperature. The permeate side was maintained at atmospheric pressure. The flux of the permeated gas was measured by a bubble flow meter and the Permeability coefficient calculated three times for each membrane. The error for the absolute values of the permeability coefficients can be estimated to about $\pm 5\%$, due to uncertainties of the determination of the gas flux and the effective membrane area and thickness, while the reproducibility is better than $\pm 4\%$. The typical membrane area in the test cell was 11.3 cm^2 . The gas permeability of membranes was determined using the following equation.

$$J = \frac{V}{At\Delta p} \cdot \frac{273.15}{T_0} \cdot \frac{P_0}{76}$$

Where J is the membrane permeance [$\text{cm}^3(\text{STP})/(\text{cmHg})$], V is the volume (cm^3) of the permeate collected at ambient conditions (temperature $T_0(\text{K})$ pressure $p^0(\text{cmHg})$) over a period of time (s), A the effective area of the membrane (cm^2), Δp the trans membrane pressure difference (cm Hg) and t is the thickness of membrane. Permeance is customarily expresses in the unit of GPU, ($1\text{GPU}=10^{-6} \text{ cm}^3(\text{STP})/\text{cm}^2 \cdot \text{s} \cdot \text{cmHg}$). The membrane permeability (P) is equal to permeance multiplied by the effective thickness of the membrane. The ideal selectivity, A/B (the ratio of single gas permeabilities) of membranes was calculated from pure gas permeation experiments:

$$\alpha \frac{A}{B} = PA/PB$$

3. Results and discussion

3.1. Characterization

FTIR spectra of 4,4'-methylene dicyclohexyl diisocyanate (H_{12} MDI), 1, 6-hexamethylene diisocyanate (HDI) Polycaprolactone diol, polyurethane prepolymer, 1,4-Butane diol, and final polyurethane are shown in Fig 2(a-e). The H_{12} MDI (2a) and (HDI) are collectively shown in (Fig. 4.1a) the very strong peak located at 2262.3cm^{-1} and 2254.5cm^{-1} are attributed to the isocyanate (NCO) group in the structure. The peaks observed in the Polycaprolactone diol (2b) are as follows 3437.1cm^{-1} (OH stretching vibrations); 2942.8cm^{-1} (asymmetric CH_2 stretching); 2866.6cm^{-1} (symmetric CH_2 stretching) 1727.1cm^{-1} ($\text{C}=\text{O}$ stretching) 1166.7cm^{-1} (C-O stretching). After 1 hour from the reaction of diisocyanates and PCL diol in the reaction vessel it was found that the NCO peak disappearance and now peak at 3363.6cm^{-1} is appeared (Fig2c). The other peaks are assigned as: 2925.8cm^{-1} (CH symmetric stretching of CH_2); 2856.4cm^{-1} (CH asymmetric stretching of CH_2); a large band issued having an intense peak at 1717.5cm^{-1} ($\text{C}=\text{O}$ stretching) of soft segment of polyol. Evidence that the polymerization reaction has been attained completely. The hydrogen bonding between carbonyl groups and urethane N-H groups in hard segments bands will correspond to those groups that are in the interior of hard segments, while the free bands may correspond to those groups in the hard segment domains or in the soft domains or at the interface. After the preparation of NCO terminated prepolymer the 1, 4-BDO as chain extender was added into the reaction mixture. The FTIR spectra of 1, 4-butanediol (Fig. 2d) has prominent bands at 2833.73cm^{-1} and 2779.72cm^{-1} attributed to the symmetric and asymmetric stretching of the CH_2 groups, respectively. The broad band appeared at 3300.0cm^{-1} is due to hydroxyl group. By extending the prepolymer with the chain extender, FTIR spectra (Fig.2e) showed a very strong peak for NH at about 3355.9cm^{-1} , the other peaks in the spectra are accredited as 2860.2cm^{-1} ; 2930.6cm^{-1} (antisymmetric and symmetric vibrations of CH groups); 1732.4cm^{-1} ($\text{C}=\text{O}$ stretching); 1690cm^{-1} (CNH stretching)¹⁴. This observation indicates more hydrogen bonding among urethane carbonyl groups and urethane N-H groups in hard segments. The numbers of imide ring structures of PU are decreased, which is due to part of PU with free NCO content reacted with -NH group of amide (-CO-NH-) chain. This is evidence that the entire NCO group has been consumed and there is no free NCO group in the final polyurethane sample and hence, Polyurethanes membranes were able to promote higher

degrees of phase compatibility¹⁵. The appearance of NH at 3355.9 cm^{-1} , CNH at 1683 cm^{-1} and disappearance of NCO at 2265.5 cm^{-1} and C=C are evidence of synthesis of polyurethane membranes.

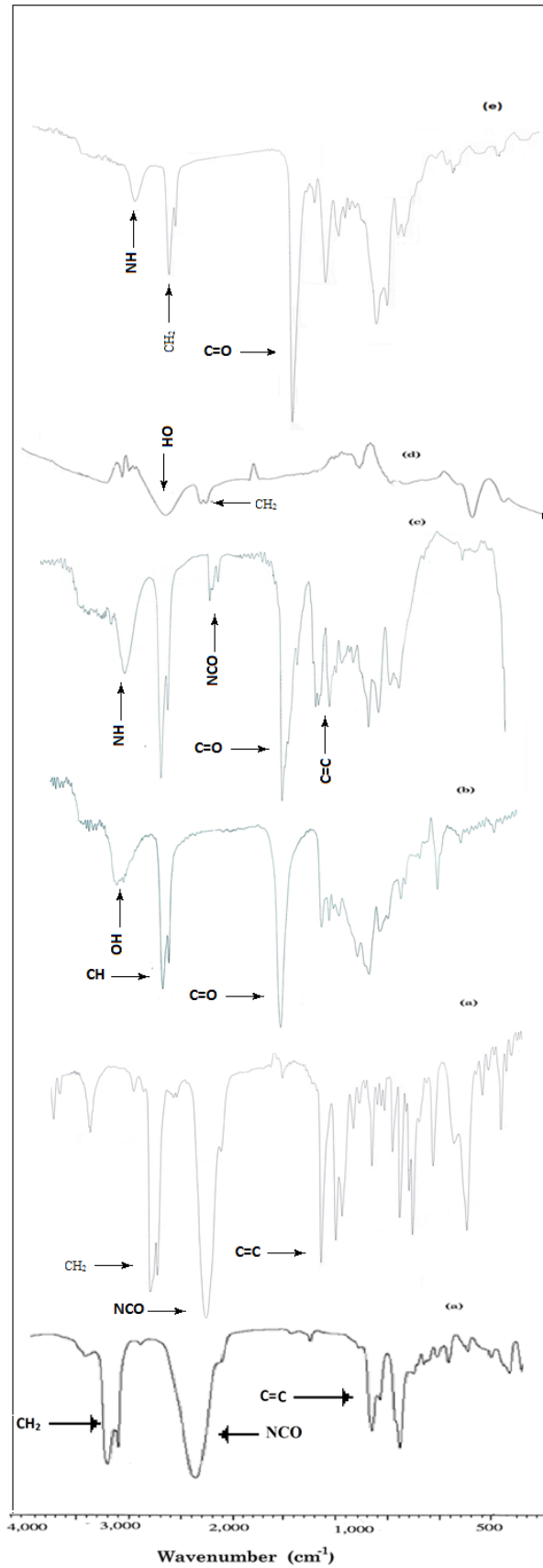


Fig2: FT-IR spectra (a)1,6-Hexamethylene diisocyanate (HDI) (a) 4,4'-methylene dicyclohexyl diisocyanate (H₁₂MDI) (b); Polycaprolactone (PCL); (c) NCO terminated Polyurethane Prepolymer (d) 1,4-Butane diol; (e) Final polyurethane membrane

3.1.2. Contact angle and swelling measurements

Contact angle analysis provides information about molecular mobility at water /solid interface on membrane surface. The result presented in the table3.1 the water contact angle was for HDI is 86θ with lower surface energy while the H₁₂MDI has 72θ but it has high surface energy. Due to existence of polar ester groups incorporating in the polymer chain groups and lack of spatial hindrance increasing hydrophilicity^{16,17}.. The swelling property of membrane with water is due to the hydrogen bonding present between polymer matrix and water¹⁷. The water absorption rate is controlled by both diffusion and polymer chain separation, which increases due to electrostatic repulsion.

Table3.1. surface properties of polyurethane membrane

Sample code	Degree of swelling at equilibrium (%)	Contact angle (θ) (Water)	Surface energy(mN/m)
HDI	0.3	86.0±0.3	77.87
H ₁₂ MDI	0.14	72.0±0.3	95.29

3.1.3. Thermal and mechanical analysis

Thermogravimetric analysis was used to study the thermal stability of polyurethane membranes. The TG curves of the sample Figure 3 gives the TGA thermograms of membranes samples in this study. The membrane HDI, H₁₂MDI state the temperature at which 10% (T_{10%}) weight loss occurs at 226°C, and 300°C, and maximum decomposition around 520°C, and 550°C,

respectively. where are two stages of degradation, in the first stage the degradation is caused by the breaking of the hard segments, because the first transition is related to soft segments, this transition occurs in the range of 50°C to 100°C¹⁸. The second stage of PU decomposition is corresponding to the breaking of urethane bond and decomposition of polyol, respectively¹⁹. The hydrogen bonding of the ether groups to urethane NH groups' decrease, but the total mobility of the soft segments does not change significantly. Thermal properties of polyurethanes are influenced by the molecular weight between the cross-linking points, the ratio and separation between hard segment domains and soft segments domains, the reinforcing fillers, and elastically active branch points^{20,21,22}. The decrease in tensile strength in HDI attributed to the decrease in hydrogen bonding. Changing diisocyanate in the polymer structure causes increasing phase separation and reduction in Tg values. In H₁₂MDI this behavior can be endorsed to increased intermolecular forces associated with the higher hard segment for the same NCO/OH ratio and highest hydrogen bonding²³.

Table3.1.3 mechanical properties of polyurethane membrane

Sample code	T ₁₀ (°C)	T ₂₀ (°C)	T ₄₀ (°C)	T ₆₀ (°C)	T ₈₀ (°C)	T _{max} (°C)	Tg (°C)	Tensile strength(MPa)	Elongation at break (%)	Hardness shore A
HDI	226	320	400	435	480	520	68	14.26	461	70
H ₁₂ MDI	300	420	445	450	500	550	50	20	300	80

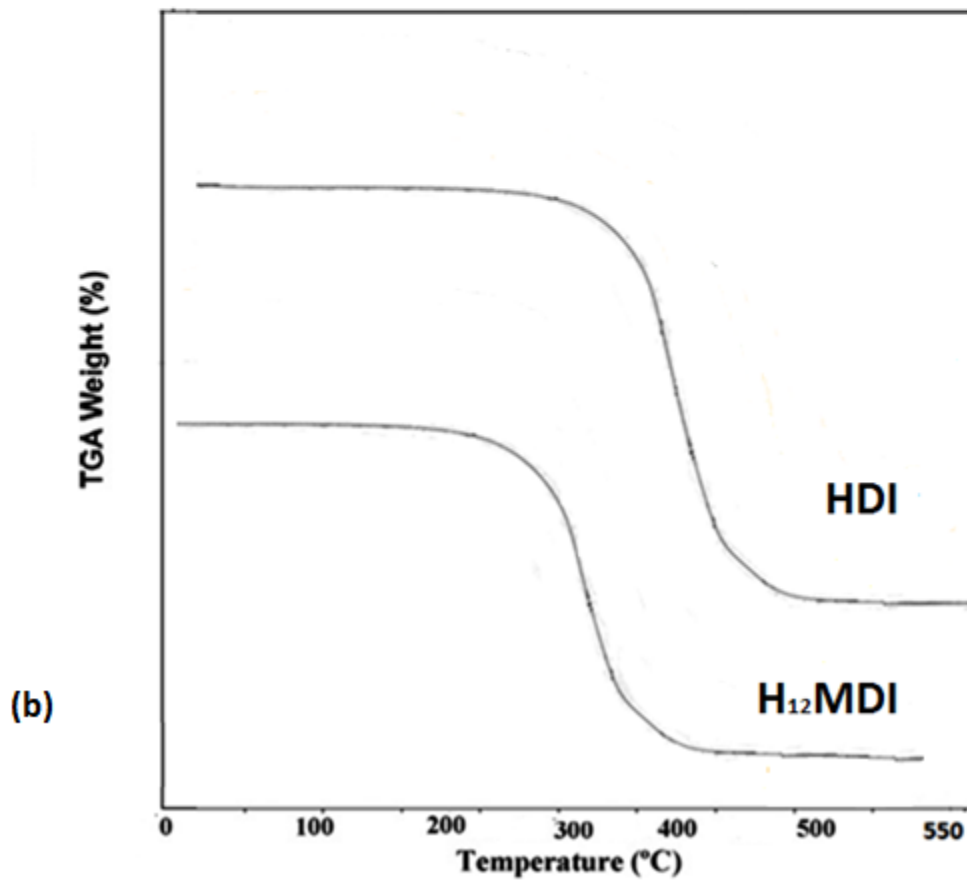
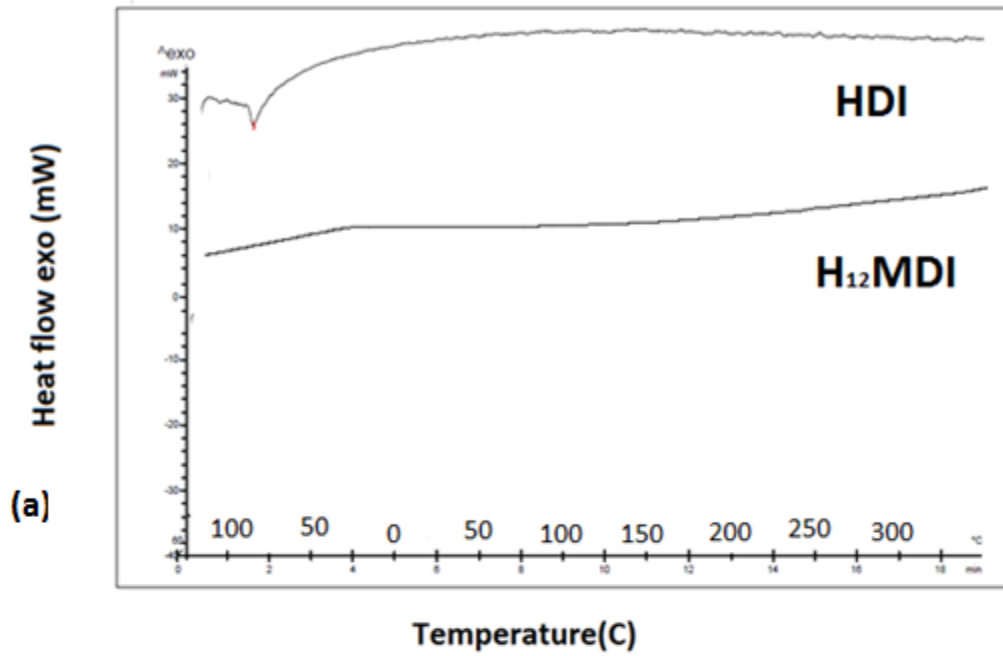


Figure 3 (a) DSc and (b) TGA scans of polyurethane membranes

Afm scanning

Figure4 (a and b) show the images of two dimensional scans of the membranes, where all prepared membranes show asymmetric structure. The structure of membrane is often described in terms of presence or absence of connecting voids. General structure was very similar for all the membranes consisting of a top dense skin layer and porous sub-layer²⁴. The porous sub-layer consists of finger-like structure. The addition of a high molecular weight component changes drastically the structure of the membranes pores are well interconnected and macrovoid formation is suppressed. The reason for such type of surface morphology may be explained from the concept of quaternary phase diagram of membrane formation. The formation of the top surface is possibly due to demixing of the casting solution leading to the formation of finger-like cavities in the sub layer of prepared membranes, i.e. the solid. The observed AFM images implied the existence of a micro-phase separation in the PU membranes. Surface morphology can be explained from the concept of quaternary phase diagram of membrane formation.

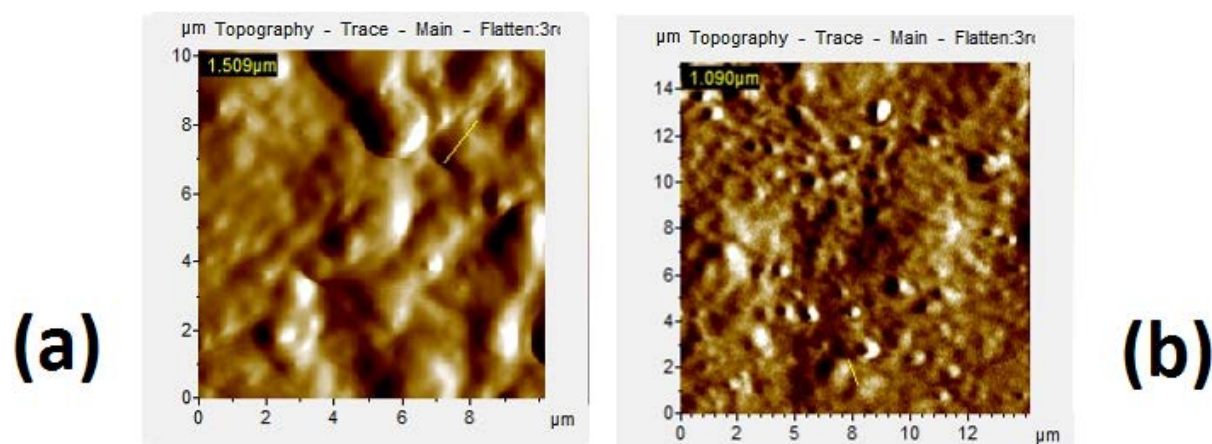


Figure 4 surface scanning of PU membranes with different diisocyanates (a) HDI (b) H₁₂MDI

3.2. Factors affecting membrane performance

3.2.1 Effect of diisocyanate addition

Comparison of gas permeability of two types of diisocyanate based polyurethane shows that gas permeability of PUs based on HDI is at maximum and permeability of PUs based on H₁₂MDI is at minimum. For membranes, the permeability decreases in the order of (CO₂) > (O₂) > (CH₄) > (N₂). The higher CO₂ permeability is related to the higher solubility of CO₂ in the membranes compared to O₂, CH₄, and N₂. Where, CO₂ has a small molecular size and a high critical temperature compared to the other gases²⁵. It is noteworthy that, CO₂ is a polar gas that can interact with polar chain polymers. Hence, the permeability of CO₂ in comparison with the gases input that contain polar groups in the main chain of the polymer is considerably higher. The permeability of CH₄ is higher than N₂ although CH₄ has a higher molecular size; its higher permeation relative to N₂ confirms the domination of the solubility mechanism in the transport of gases through polyurethane membranes. In HDI based PUs, membranes due to more phase separation, hard segments have no interfere with soft segments thus soft segments have enough space and mobility to create ordered and crystalline structures. The main reason for more phase separation in PUs containing HDI has ability to pack and find ordered structures in their hard segments as compared to H₁₂MDI.

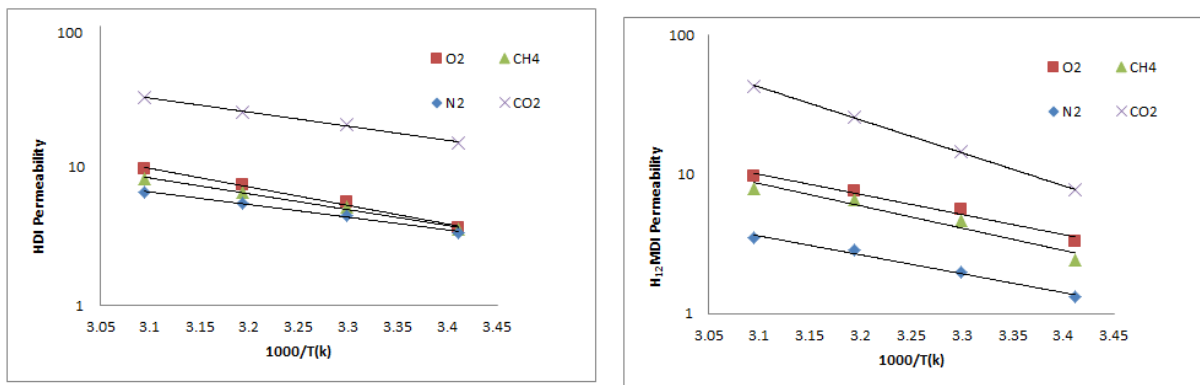


Figure 5 effect of diisocyanate on gas permeability

3.2.2 Effect of Temperature

To study the effect of temperature on the gas permeance and selectivity, the polyurethane membranes were tested for O₂, N₂, CH₄ and CO₂ permeation at temperatures ranging from 20 to 50°C at constant transmembrane pressure, 0.4 MPa. The gas permeability of PUs based on HDI is at maximum and permeability of PUs based on H₁₂MDI is at minimum with the increase of

temperature. The permeance of gases increase with increase of temperature, and the temperature dependence of the permeance appear to follow an Arrhenius type of relationship. Permeability of methane is more than nitrogen in despite of its higher molecular size. The oxygen with lower molecular size has high permeability as compared to methane and nitrogen. This might be due to presence of (-COO-) polar groups in soft segments that leads to decreasing phase separation between soft and hard segments which in turn reduces the rubbery properties of the polymer²⁶. However, N₂ permeance is affected by temperature more significantly; resulting in the reduction of CO₂/CH₄ selectivity in HDI based PU membrane when temperature increases. According to solution-diffusion mechanism the permeation of gases through polymeric membranes, the permselectivity of a gas pair is composed of solubility and diffusivity selectivity of the gases in membrane²⁷. The molecular sieve property also plays an important role in the slightly enhancement of permselectivity of CO₂/CH₄, CO₂/N₂, CH₄/N₂ and O₂/N₂, gases in H₁₂MDI based PU membranes. In the case of O₂/N₂, the low selectivity is due to the condensabilities of these two gases are very low and not very different, the molecular size difference in this pair of gases plays an important role. The decreased mobility of polyol chains in soft segment and ultimately increased diffusion selectivity. Increasing phase separation leads to an increase in rubber properties of the PUs that causes the increase of the free volumes and gas solubility in this polymer membrane. The CO₂/N₂ selectivity in H₁₂MDI PUs is little bit higher. Because the permeation of more condensable CO₂ gas in comparison to nonpermeable nitrogen increase in more phase separated structures, therefore effect of the solution selectivity in the separation of condensable and non-condensable gases increase and this membrane show the higher CO₂/N₂ selectivity in comparison to the HDI system.

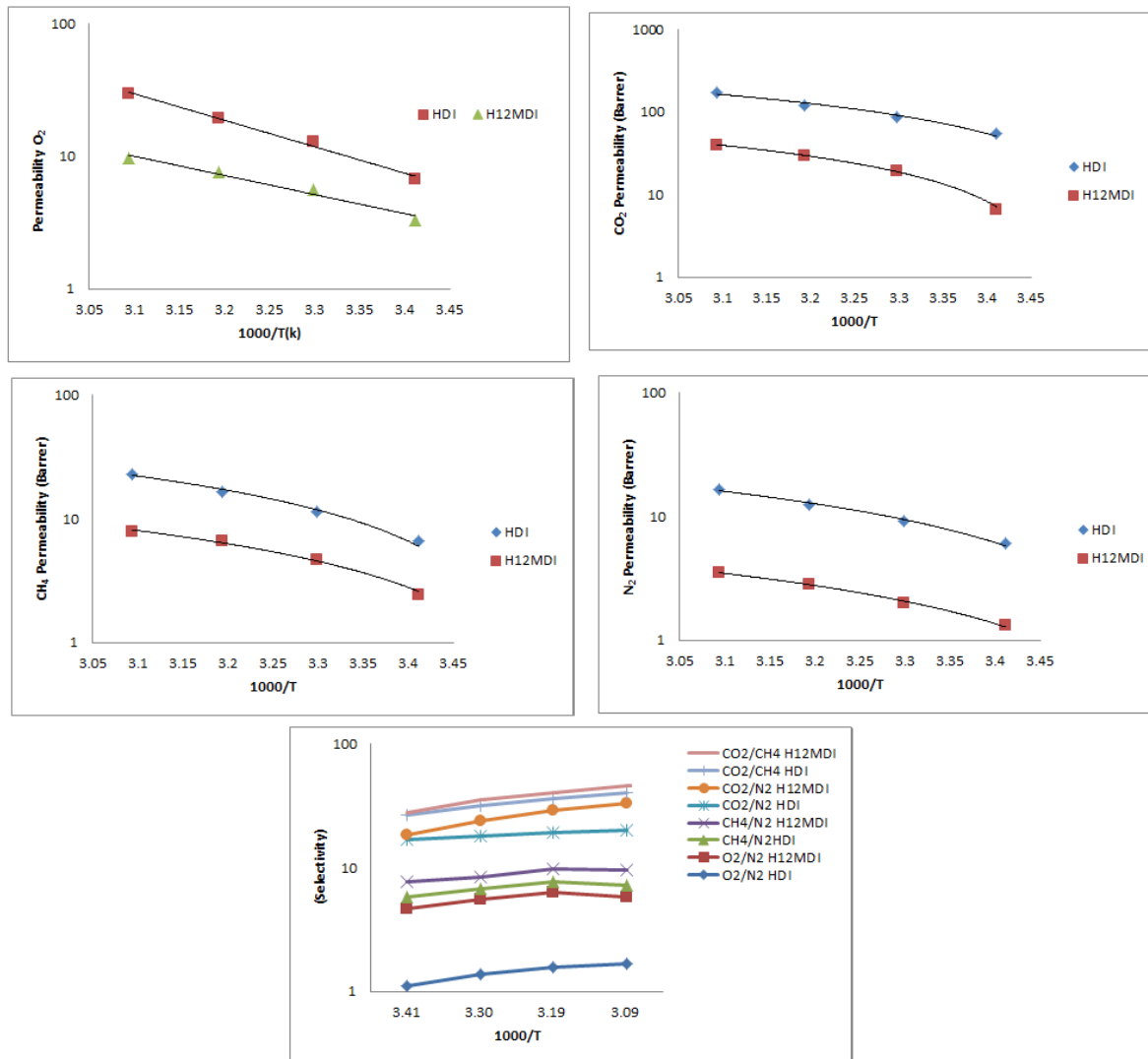


Figure6 Temperature dependences permeability and selectivities of PU membranes

3.2.3 Effect of pressure

To investigate the effect of pressure on the gas permeability, membranes containing 2000 molecular weight of PCL were tested at 50°C temperature and different cross membrane pressure (0.1, 0.2, 0.3, 0.4MPa). As illustrated in graphs, 7 the permeability coefficients for N₂, O₂, and CH₄ are independent of pressure and increased in HDI based polyurethane membranes. But the overall permeation of gases through all polyurethane membrane increased slightly with an increase in pressure. It has been concluded that the effect of the operating pressure on the gas permeability for PU membranes is not significant. In comparisons, CO₂ permeability coefficients increase significantly with increasing feed pressure, whereas the permeance of N₂ decreased

more significantly, resulting in a lesser extent of increase in the ideal separation factor for CO₂/N₂ permeation in HDI. O₂/N₂, CH₄/N₂ gas pair selectivity is enhanced in HDI based polyurethane membrane with the increase of pressure. The reason might be that at higher pressure, the polymer segments have greater flexibility and the membrane is compressed more as compared to when different temperature is applied. The Figure7 shows that the ideal separation factors of CO₂/CH₄ and CO₂/N₂, gases these gas pairs are of interest for flue gas separation and natural gas upgrading. The membrane selectivity is not significantly influenced by the gas pressure in the pressure range tested. The high CO₂/N₂ permselectivity data imply that the H₁₂MDI based polyurethane membrane can be used to separate CO₂ from flue gas.

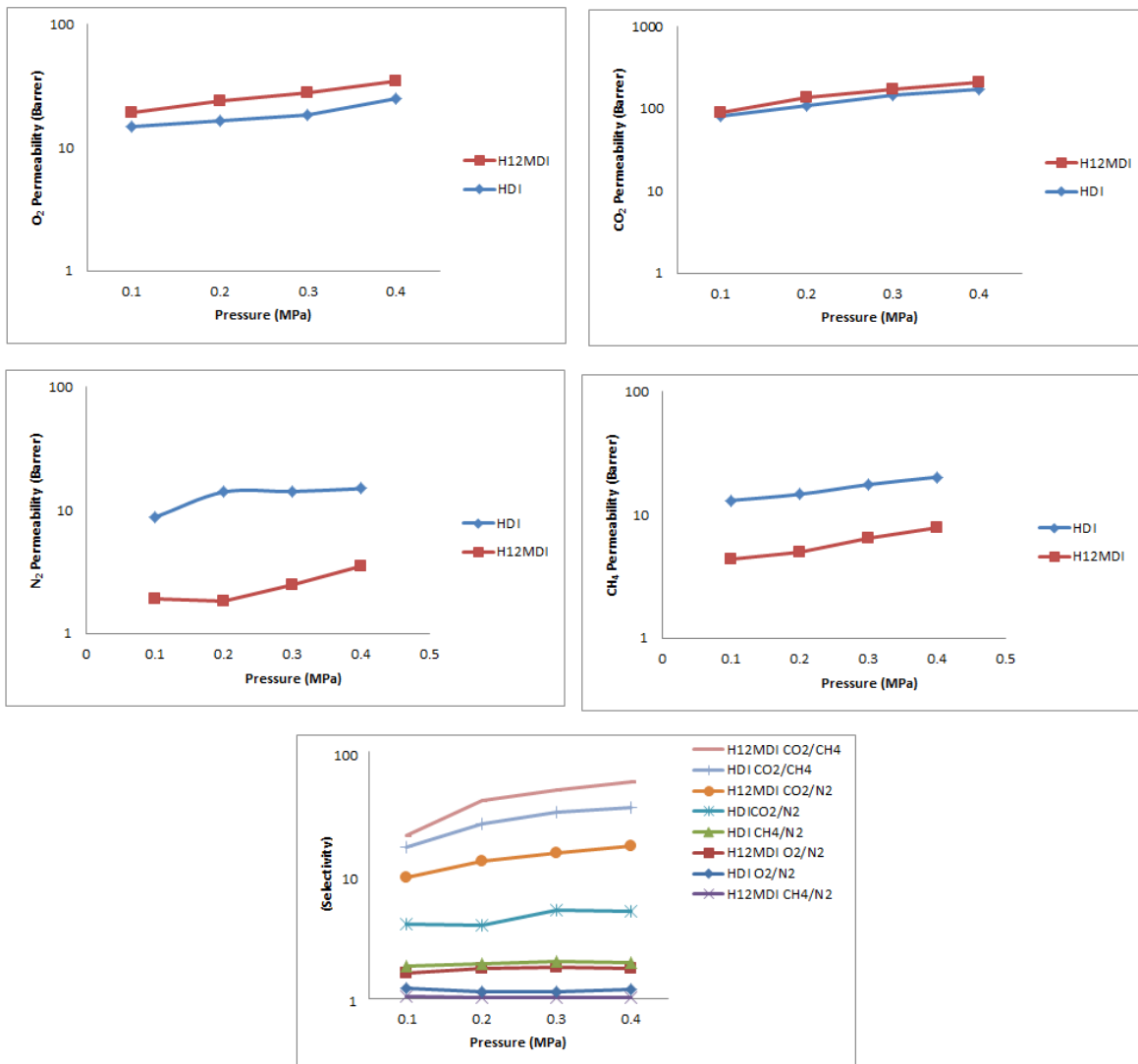


Figure7 Pressure dependences permeability and selectivities of PU membranes

4. Conclusions

The physical and permeation properties of prepared PU membranes with different diisocyanate were determined. From results it is concluded that the membranes has high permeability and there is slight selectivity difference between these two membranes. The permeance of gases increase with increase of temperature resulting in the reduction of CO₂/CH₄ selectivity in HDI based PU membranes. But, the CO₂/N₂ selectivity in H₁₂MDI PUs is little bit higher. This difference is due to the reduction of chain mobility and flexibility of soft segments and may be also due to the reduction of free volume in the membrane due to the presence of hard segment. Polar functional groups like ether oxygen are mandatory to improve or facilitate interactions between acidic gases or condensable large hydrocarbon molecules.

1. Barrer, R.; Barrie, J.; Slater, J., *Journal of Polymer Science* 27, 177 1958.
2. Van Amerongen, G. J., *Journal of Applied Physics* 17, 972 1946.
3. Barrer, R.; Skirrow, G., *Journal of Polymer Science* 3, 549 1948.
4. Donohue, M.; Minhas, B.; Lee, S., *Journal of membrane science* 42, 197 1989.
5. Scholes, C. A.; Chen, G. Q.; Stevens, G. W.; Kentish, S. E., *Journal of Membrane Science* 346, 208 2010.
6. Park, H. B.; Jung, C. H.; Lee, Y. M.; Hill, A. J.; Pas, S. J.; Mudie, S. T.; Van Wagner, E.; Freeman, B. D.; Cookson, D. J., *Science* 318, 254 2007.
7. Lin, H.; Freeman, B. D., *Journal of Membrane Science* 239, 105 2004.
8. Zia, K. M.; Barikani, M.; Bhatti, I. A.; Zuber, M.; Bhatti, H. N., *Journal of applied polymer science* 109, 1840 2008.
9. Weibel, D. E.; Vilani, C.; Habert, A. C.; Achete, C. A., *Journal of Membrane Science* 293, 124 2007.
10. Semsarzadeh, M. A.; Ghalei, B., *Journal of Membrane Science* 432, 115 2013.
11. Wolińska-Grabczyk, A.; Żak, J.; Jankowski, A.; Muszyński, J., *Journal of Macromolecular Science, Part A* 40, 335 2003.
12. Faria, M.; Rajagopalan, M.; de Pinho, M. N., *Journal of Membrane Science* 387–388, 66 2012.
13. Chattopadhyay, D.; Webster, D. C., *Progress in Polymer Science* 34, 1068 2009.
14. Sadeghi, M.; Afarani, H. T.; Tarashi, Z., *Korean Journal of Chemical Engineering* 32, 97 2015.
15. Ayres, E.; Vasconcelos, W. L.; Oréface, R. L., *Materials Research* 10, 119 2007.
16. Mândru, M.; Ciobanu, C.; Vlad, S.; Butnaru, M.; Lebrun, L.; Popa, M., *Central European Journal of Chemistry* 11, 542 2013.
17. Zhou, D.; Choi, P., *Polymer* 53, 3253 2012.
18. Saucedo-Rivalcoba, V.; Martínez-Hernández, A.; Martínez-Barrera, G.; Velasco-Santos, C.; Castaño, V., *Applied Physics A* 104, 219 2011.

19. Chen, C.-J.; Tseng, I. H.; Lu, H.-T.; Tseng, W.-Y.; Tsai, M.-H.; Huang, S.-L., *Materials Science and Engineering: A* 528, 4917 2011.
20. Yampolskii, Y., *Macromolecules* 45, 3298 2012.
21. Dusek, K.; Spirkova, M.; Havlicek, I., *Macromolecules* 23, 1774 1990.
22. Khosravi, A.; Sadeghi, M.; Banadkahi, H. Z.; Talakesh, M. M., *Industrial & Engineering Chemistry Research* 53, 2011 2014.
23. ZIA, K. M.; BARIKANI, M.; BHATTI, I. A.; ZUBER, M.; BHATTI, H. N., *Journal of applied polymer science* 109, 1840 2008.
24. Aminudin, N. N.; Basri, H.; Sean, G. P.; Hubadillah, S. K.; Rosman, N., *Australian Journal of Basic & Applied Sciences* 82014.
25. Sadeghi, M.; Semsarzadeh, M. A.; Barikani, M.; Pourafshari Chenar, M., *Journal of Membrane Science* 376, 188 2011.
26. Saedi, S.; Madaeni, S. S.; Hassanzadeh, K.; Shamsabadi, A. A.; Laki, S., *Journal of Industrial and Engineering Chemistry* 20, 1916 2014.
27. Sadeghi, M.; Semsarzadeh, M. A.; Barikani, M.; Ghalei, B., *Journal of Membrane Science* 385–386, 76 2011.